FOLR2 transfer by trogocytosis from nurse-like cells to CLL cells is linked to their activation and proliferation

Marcin Domagala[1], Chloe Bazile[1], Bastien Gerby[1], Loïc Ysebaert[1,3], Vera Pancaldi[1], Camille Laurent[1,2] and Mary Poupot [1*]

[1] CRCT, UMR1037 Inserm-Univ. Toulouse III Paul Sabatier-ERL5294 CNRS, 2 avenue Hubert Curien Oncopole de Toulouse, CS53717, 31037, Toulouse, France.

[2] Service d'anatomopathologie, Institut Universitaire du Cancer de Toulouse - Oncopôle, 31059 Toulouse, France.

[3] Department of Haematology, Institut Universitaire du Cancer de Toulouse - Oncopôle, 31059 Toulouse, France.

Corresponding authors: Marcin Domagala (marcin.domagala@inserm.fr) and Mary Poupot (mary.poupot@inserm.fr); 2 avenue Hubert Curien Oncopole de Toulouse, CS53717, 31037, Toulouse, France. Phone : +335 82 74 16 62, fax: +335 82 74 16 85.

ABSTRACT

Neoplastic B cells in chronic lymphocytic leukemia (CLL) are particularly dependent on the tumor microenvironment (TME) located in lymphoid organs. Contact with microenvironment facilitates survival, proliferation and resistance to treatment of CLL cells. Here, we studied the interaction between CLL cells and nurse-like cells (NLCs), a subtype of macrophages heavily implicated in the pathogenesis of this disease. Using *in vitro* cultures of human primary cells, we demonstrated that NLCs express high levels of folate receptor beta (FOLR2), which correlates with survival of CLL cells. Next, we discovered that CLL cells acquire functional FOLR2 from the NLCs through trogocytosis, thereby increasing their uptake of folates. Treatment of CLL and NLC co-cultures with IL-15 and CD40L, to mimic TME, substantially increases the frequency of FOLR2$^+$ CLL cells, which are significantly enriched in activated and proliferating fraction of the cells, particularly under folic acid depletion. With multi-immunofluorescence analysis of CLL patients' lymph nodes, we confirmed the presence of FOLR2$^+$ NLCs, whose frequency correlates with increased proliferation of cancer cells. Further detection of FOLR2$^+$ CLL cells, provided evidence of trogocytosis in vivo. Finally, based on CD163/FOLR2 co-staining and spatial distribution of NLCs we uncovered heterogenous subpopulations of these cells suggesting their various specialization. This work proposes trogocytosis as an important mechanism of NLC-dependent support of CLL cells, and underscore FOLR2 as a new marker of NLCs. It paves a way to further study the impact of trogocytosis on progression of CLL and beyond.

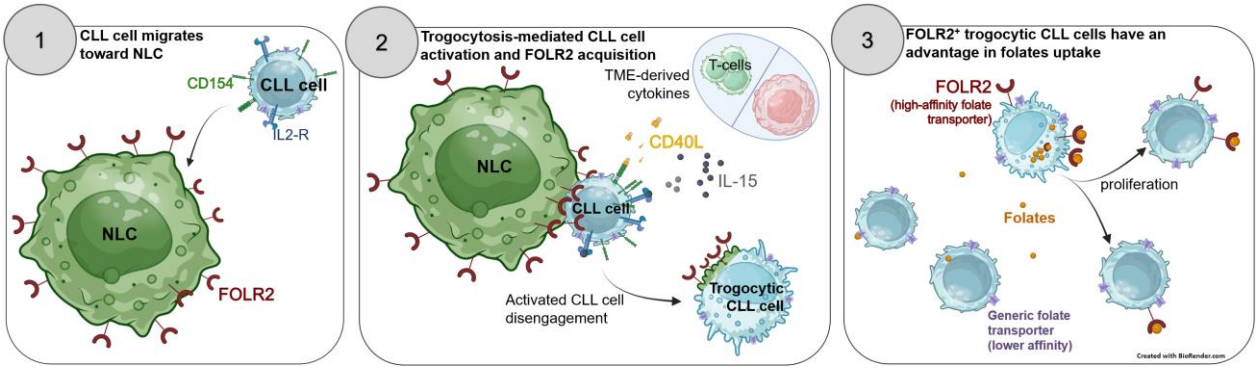

Scheme 1 Schematic representation of trogocytosis-mediated acquisition of NLC-derived FOLR2 by CLL cells promotes cancer cells adaptability and proliferation. 1) CLL cells enter the lymph node (LN) and engage in contact with FOLR2$^+$ NLCs. 2) The presence of T cell- and stromal cell-derived cytokines, CD40L and IL-15 promotes the activation and trogocytosis-mediated acquisition of FOLR2 by CLL cells. 3) FOLR2$^+$ trogocytic CLL cells have an advantage in folate acquisition and show increased proliferation compared to the remaining population of cancer cells

SUMMARY

- FOLR2 is a marker of M2-like protective NLCs
- CLL cells acquire functional FOLR2 from NLCs through trogocytosis, allowing them to enhance folate uptake
- Trogocytic FOLR2$^+$ CLL cells are enriched in the fraction of activated and proliferative cells, especially during folic acid scarcity
- Discovery of FOLR2$^+$ NLCs and FOLR2$^+$ trogocytic CLL cells in the LNs of CLL patients.

INTRODUCTION

Chronic lymphocytic leukemia (CLL) is the most common B cell malignancy of western countries, characterized by the clonal accumulation of dysfunctional, $CD5^+$ mature-like B cells in peripheral blood (PB) and lymphoid organs, including bone marrow (BM) or lymph nodes (LNs)[1]. CLL cells in periphery are mostly quiescent, and migrate to lymphoid organs, where they proliferate thanks to specific microenvironment [1]. CLL microenvironment is also critical for cancer cell survival and chemoresistance[2–6] facilitating a contact with T cells, endothelial cells, mesenchymal stromal cells and nurse-like cells (NLCs)[1,7]. NLCs were first observed in the *in vitro* CLL PBMC cultures [8,9], and described as a monocyte-derived population of $CD68^+$, $CD163^+$ macrophages, interacting closely with CLL cells and protecting them against spontaneous apoptosis [8,9], and therapeutic attacks[10–12]. Moreover, NLCs are crucial for attracting cancer cells to the lymphoid organs[1], and their increased numbers in the LNs and infiltration into proliferation centers correlates with more aggressive disease[4] and shorter overall survival[4,13].

NLCs protect CLL cells through the release of soluble factors and direct contact. While the effect of NLCs' secretome on CLL cells has been widely appreciated[1,5,7,14], the role of direct contact, requires further study. For instance, vimentin and calreticulin presented by NLCs, serve as antigens for CLL cells B-cell receptors (BCRs), inducing their activation, and in turn survival and potentially proliferation[7,15]. Direct contact between NLCs and CLL cells mediated through CD31 on NLCs and CD38/CD100 on CLL cells is implicated in proliferation of $CD38^+/CD100^+$ malignant clones[16]. Moreover, our group showed that trogocytic interaction, partially mediated through CD2/CD58 (LFA-3) is essential in promoting cancer cell survival *in vitro*[17]. Trogocytosis is a type of direct cell interaction, where one cells nibbles another, leading to the rapid acquisition of cellular content, including integral plasma membrane fragments[18]. This process is predominantly unidirectional, enabling recipient cells, among others, to acquire new functionalities and modulate immune responses. Trogocytosis is an evolutionary-conserved process, implicated in both physiology and pathology [18–20]. However, its role in cancer, including CLL, especially in the context of malignant cell interactions with TME remains poorly understood[21].

In recent years, folate receptor β (FRβ/FOLR2) emerged as a specific marker of TAMs [22–24]. FOLR2 belongs to a family of folate receptors characterized with high affinity to folates. FOLR2 expression is restricted to myeloid cells, particularly the M2-like immunosuppressive subpopulation of macrophages[25]. FOLRs along with two other receptors (RFC and PCFT) are the main receptors responsible for uptake of folates (vit. B9)[26]. Folates, including synthetic folic acid, are essential co-factors for one-carbon metabolism, necessary for nucleic acid synthesis, amino acid homeostasis, epigenetic modifications and redox defense[27].

The aim of this study was to further characterize NLCs and their interaction with CLL cells. We showed for the first time that NLCs express high levels of FOLR2, which serves as a distinctive marker of the protective phenotype of these cells. Moreover, we demonstrated that CLL cells engage in trogocytic interactions with NLCs, leading to the acquisition of functional FOLR2. As a result, trogocytic $FOLR2^+$ CLL cells show increased capacity for folate uptake, and are significantly enriched in the fraction of activated and proliferating cells *in vitro*. Analysis of CD163 and FOLR2 expression in CLL patientLNs revealed previously unknown heterogeneity of NLCs, demonstrated association of $FOLR2^+$ NLCs with cancer cells proliferation and allowed detection of $FOLR2^+$ trogocytic CLL cells. These results stress the importance of trogocytosis in the NLC-CLL interactions, while FOLR2 acquisition by CLL cells represents a novel mechanism of NLC-mediated support of malignant B cells.

MATERIALS AND METHODS

Cell preparation and culture

Peripheral blood samples from CLL Patients were obtained from the Hematology Department with informed consent and referenced in the INSERM cell bank. According to French law, the INSERM cell bank has been registered with the Ministry of Higher Education and Research (DC-2013-1903) after being approved by an ethics committee (Comité de Protection des Personnes Sud-Ouest et Outremer II). Clinical and Biological annotations of the samples have been reported to the Comité National Informatique et Liberté.
Blood samples from CLL patients or healthy donors' buffy coats (EFS France) were used for PBMC isolation by density-gradient centrifugation. Isolated PBMC were used directly for the downstream processing or frozen for further use.

Cell isolation
CLL cells were isolated from PBMC, using a EasySep™ Human B Cell Enrichment Kit II Without CD43 Depletion negative selection kit (STEMcell, France), according to manufacturer's protocol. Purity and viability of the cells after isolation were measured by flow cytometry following staining with CD5/CD19 antibodies and Annexin-V/7-AAD respectively. For each experiment, both values exceeded 95% (data not shown).
Healthy donor monocytes: following a buffy coat processing (EFS - Établissement français du sang, France), PBMC were subjected to CD14 MicroBeads positive selection kit with use of MS/LS columns (Miltenyi Biotec, France), according to the manufacturer's protocol. Eluted cells were stained with anti-CD14 mAb and analyzed by flow cytometry confirming >95% purity of the cells (data not shown). Isolated monocytes were used freshly for generation of monocyte-derived macrophages (MDM) or healthy donor NLCs (HD-NLCs).

Cell cultures
Cells were culture in RPMI 1640 with GlutaMAX + 10% FBS and 100 µg/ml of penicillin/streptomycin *In vitro* cultures were conducted using complete medium, composed of RPMI 1640 with GlutaMAX (Gibco, France), supplemented with 10% fetal bovine serum (FBS, Life Technologies, France) and 100 µg/ml of penicillin/streptomycin (Sigma-Aldrich, France). For experiments with varying concentration of folic acid (FA), media were prepared on the basis of RPMI 1640 without folic acid (Gibco, France) and 100 µg/ml of penicillin/streptomycin. For FA^{high} condition, the media was supplemented with FA up to standard concentration of 2.27µM. Subsequently, both FA^{high} and FA^{low} media were supplemented with 10% FBS. For $FA^{negative}$ condition, 10% of dialyzed FBS (Sigma, Germany) was used instead. Cells were plated in tissue culture-treated plates (Corning, USA) at varying volumes: 4 mL per well for 6-well plates, 1.5 mL per well for 12-well plates, and 500 µl per well for 48-well plates. All cultures were maintained at 37°C in a humidified atmosphere with 5% CO2.
Freshly isolated CLL PBMCs were plated at 10×10^6 cells/mL and cultured for 15 days. Floating cells were collected by pipetting, while adherent detached with Accutase. Combined fractions of the cells were used for NLCs analysis. Monocyte-derived macrophage were generated from healthy donor monocytes after CD14+ isolation. CSF1 or GM-CSF were used for initial differentiation of M2- or M1-MDMs respectively. IL-4 and IL-13 were used for subsequent M2 polarization, while IFNγ and LPS for M1 polarization.

Healthy-donor NLC (HD-NLC) co-culture system

Basic protocol: $CD14^+$ healthy donor monocytes at 0.5×10^6 c/mL were mixed with naïve purified CLL cells at 10x106c/mL in 500 µL of complete medium. After 10 days of co-culture, cells were activated with either a CpG + IL-2 cocktail or a CD40L + IL-15 cocktail for 72h and CLL cells were analyzed by flow cytometry.

Optimized Protocol: MDMs were generated by culturing $CD14^+$ cells at 1×10^6 cells/mL in 250uL of complete medium with 20ng/mL of CSF-1. After 6 days, the medium was replaced, and purified naïve CLL cells were added at a density of 6×10^6 c/mL in 250 µL of complete medium. 3 days later, 250ul of fresh medium with CD40L to a final concentration of 25ng/mL was added to the co-cultures. 2 days after the first activation, 300 µL of the medium was replaced, and cells were further activated with CD40L and IL-15 to final concentrations of 50 ng/mL and 25 ng/mL, respectively. 6 days post-second activation, cells were analyzed by flow cytometry.

FOLR2 gene KO in hNLCs with RNP Crispr-Cas9

Gene KO in HD-NLCs cultures were achieved using ribonucleoprotein (RNP)-mediated CRISPR-Cas9 gRNA method, using predesigned crRNA sequences (Integrated DNA Technologies; IDT). For the target gene, three different crRNA targeting both alleles of the coding regions gene were used. 16h before electroporation, monocytes were activated with 25 ng/mL of CSF-1 and cultured in the medium without antibiotics. RNP complexes were performed according to provider's instruction (IDT) using Neon Transfection System, with a single pulse at 1900V and 20ms. Following electroporation, cells were plated in the complete medium. 90 min later, the cell culture media was replaced with a fresh one containing 20 ng/mL of CSF-1 to remove the traces of electroporation buffer. Afterward, cells were cultured for 5 days, before starting the co-culture with CLL cells or evaluating effectiveness of gene KO by qPCR or flow cytometry.

Flow cytometry

Extracellular staining: All tested samples were suspended in the staining buffer (5% FBS, 0,5% of BSA, 2mM EDTA, 0.1% of sodium azide in PBS), supplemented with 2.5 µg/mL of Human BD Fc Block™ (BD Pharmingen, France) and 1% of human serum to prevent the non-specific antibody binding, and incubated for 15 min at 4°C. Subsequently, cells were stained with antibodies at saturating concentrations, for 20 min at 4°C. After washing, cells were re-suspended in PBS, containing 0.8 µg/mL 7-AAD (Sony, USA).

Intracellular staining: Cells were stained with FVS620 viability dye (BD) according to manufacturer's protocol. Following the extracellular staining, cells were fixed and permeabilized with True-Nuclear™ Transcription Factor Buffer Set (Biolegened). Next, cells were stained with anti-Ki67 mAb (Invitrogen).

AnnexinV/7-AAD staining of CLL cells: Cells were washed and resuspended in Annexin-V buffer and stained with Annexin-V-FITC (Miltenyi, Germany) according to manufacturer protocol. 5 minutes before the analysis, cells were resuspended in Annexin-V buffer containing 0.8 µg/mL 7-AAD.

Following each staining, cells were immediately analyzed by flow cytometry (LSRII or FortessaX20, BD Pharmingen, France).

Results analysis: All flow cytometry results were analyzed using FlowLogic 7.00.2 software (Inivai Technologies). Gating strategies for the analysis of CLL cell activation and proliferation can be found in the supplement section (Fig. S4D and S5A, respectively). Setting-up of the gates for the $FOLR2^+$ cells were set either based on isotype controls (Fig.2) or FMO controls (Fig. 4 and 5).

The analysis of the enrichment of $FOLR2^+$ trogocytic cells in the population of activated CLL cells, was made by introducing a FOLR2 enrichment score (ES_{FOLR2}), further correlated with the total percentage of CLL cells positive for a specific activation marker (Fig. S4E; A). Ki67 enrichment score was calculated analogously, to represent enrichment of $Ki67^+$ CLL cells in the population of $FOLR2^+$ trogocytic CLL cells.

Fluorescence microscopy imaging

Following the long-term culture (12-14 days), CLL PBMC were harvested and re-suspended in the staining buffer (5% FBS + 0.5% of BSA + 1mM EDTA in PBS) containing 1% of human serum and 2.5 µg/mL of Human BD Fc Block™ (BD Biosciences, France) and incubated for 15 min at 4°C. For detection of extracellular antigens, cells were directly stained with fluorochrome-conjugated antibodies anti-CD19 (Sony) and rabbit anti-FOLR2 mAbs (Abcam) for 20 min at 4°C. Subsequently, cells were washed x4 with PBS and fixed with 4% PFA in PBS for 20 min at RT. Following washing, cells were counterstained with DAPI (1µg/mL) for 5 min, washed with PBS and left on the cover glass O/N at 4°C to facilitate attachment of the cells. The next day, slides were mounted using Fluoromount media (ThermoFisher), and imaged using confocal microscope LSM 780 or 880 (Zeiss).

Trogocytosis assay

Autologous or heterologous NLCs were detached using Accutase and stained with PKH67 according to the manufacturer's protocol. Next, stained NLCs were mixed with naïve CLL cells after negative selection (ratio 1:3), transferred to 96-well Ultra-low attachment (ULA) plate and placed in the cell culture incubator at 37°C for 3 hours. Afterward, cells were stained with appropriate antibodies and analyzed by flow cytometry. We used purified naïve CLL cells, as the negative control of trogocytosis.

Immunohistochemistry

FOLR2 Immunohistochemistry: automated classical immunohistochemical (IHC) stain was performed using the BOND RX automated slide stainer (Leica Biosystems, France). Slides (4µm) were deparaffinized and heat-pretreated using the ER2 solution (pH8) during 20 min. After peroxidase blocking, slides were incubated with the rabbit primary anti-FOLR2 antibody, clone EPR25731-70 (ABCAM Netherlands, at final dilution of 1/200, Envision Flex antibody diluent, Agilent Technologies) for 15 minutes. The target is visualized using the BOND Refine DAB detection kit (DS9800, Leica Biosystems, France). Slides were counterstained using Hematoxylin (Leica Biosystems, France), dehydrated and mounted using a xylene-based mounting medium (Sakura TissueTekÒ, Sakura FineTec France).

Multiplex Immunofluorescence (mIF): the BOND RX staining platform (LEICA Biosystems, Germany) was used to automate the mIF staining procedure on 4 µm FFPE tissue sections. After baking and dewaxing, tissue slides were heat-pretreated for 20 min at 100°C using ER2 pretreatment solution (pH9, LEICA Biosystems, Germany). The slides were blocked for endogenous peroxidase activity using the Discovery inhibitor (15 minutes at room temperature) (07017944001, Roche Diagnostics, Switzerland). The slides were then stained for 5-plex immunofluorescence using the OPAL™ Technology (AKOYA Biosciences, USA) with sequential denaturation using ER1 pretreatment buffer (pH6, LEICA Biosystems, Germany), for 20 min at 97°C between each antibody-staining cycle. Primary antibodies were applied and incubated during 30 min at room temperature programmed in the aforementioned staining cycles in the following order: FOLR2 (clone EPR25731-70 (ABCAM Netherlands), at final dilution of 1/200, Envision Flex antibody diluent, Agilent Technologies), Ki67 (clone SP6, Ready to use, Zytomed, by Diagomics, France), CD163 (clone MRQ-26, Ready to use, Roche Diagnostics), CD68 (clone PGM-1, at dilution of 1/100, in Envision Flex antibody diluent) and CD20 (clone L26, Ready to use antibody diluted at ¼ in Ventana Antibody diluent, Roche Diagnostics). Subsequently, slides were incubated using the Opal polymer HRP detection system, allowing for OPAL™ dye precipitation. Five OPAL™ dyes with excitation and emission wavelengths compatible with our whole slide imaging system were used: OPAL™ Polaris 480, OPAL™ 520, OPAL™ 570, OPAL™ 620 (1/300 in 1x Plus Automation Amplification Diluent, AKOYA Biosciences, USA) and OPAL™ 690 (1/150 in 1x Plus Automation Amplification Diluent). The tissue slides were counterstained using Spectral DAPI (AKOYA Biosciences, USA) and mounted with Invitrogen™ ProLong™ Gold Antifade Mounting medium (Life Technologies, USA).

Image analysis: the mIF images were analyzed by HALO software (version 3.6, Indica Labs, USA). Briefly, each section was manually annotated, to take into consideration the maximal area of the tissue, with removing the artifacts generated during the sample preparation. Subsequently, we optimized the segmentation parameters, allowing for the most consistent cell separation, adjusting each marker to minimize the false positive events. Afterward, the annotated regions were segmented and analyzed, and obtained image data was exported as FCS file, for subsequent analysis by FlowLogic software. Each cell was classified based on the combination or the specific dye intensity and the completeness of their nuclei or cytoplasmic region. Final graphs were visualized by GraphPad Prism 10.1.2.

Statistical analysis

All statistical analyses were performed using Graph Pad Prism 10.1.2. Mann-Whitney U test was used for comparison of MFI of surface markers on NLCs and other macrophages. Paired t-test or Wilcoxon test was used to determine the differences in viability of CLL cells or MFI. One-way ANOVA with Geisser-Greenhouse correction was used to compare the results of analyzes on CLL cell viability, activation, and proliferation. Results in the bar plots are presented as mean ± SD. The lines in the middle of the boxes in the box-and-whisker plots represent median values. The p-values below 0.05 were considered statistically significant.

RESULTS

FOLR2 expression by NLCs correlates with survival of CLL cells *in vitro*

The polarization state of TAMs is determining for their role in the TME[29]. Previously, we showed that M2-like NLCs (CD163^{high}, CD14^{high}, CD209^{pos}, CD64^{low}, CD86^{low}) interact with, and support CLL cells, unlike M1-like NLCs (CD163^{low}, CD14^{low}, CD209^{low}, CD64^{high}, CD86^{high})[28]. To further define phenotype of protective NLCs, we used CLL PBMC *in vitro* culture (Fig. 1A), to perform a screening of protein markers associated with protumoral TAMs (Fig. S1A). It revealed that M2-like NLCs express high level of FOLR2 (Fig. S1A, 1B), which was not only co-expressed along CD163, a standard NLCs marker[5] (Fig. S1B), but also significantly overexpressed (MFI = 23057 vs 4268, n=9, $p<0.003$) compared to M2-like monocyte-derived macrophages (MDMs; Fig. 1C).

Next, we evaluated kinetics of FOLR2 expression in CD14^{+} monocytes differentiating into NLCs over 14 days of PBMC culture. FOLR2 signal was detectable on monocytes from day 3, peaking at days 9-10 for patient samples P1-3, but diminishing completely towards the end of the culture for P4-6 (Fig. 1D). Moreover, for P1-3 (FOLR2^{high} NLCs) CLL cells survival on day 14 exceeded 90%, whereas for P4-6 (FOLR2^{neg} NLCs) dropped below 65% (Fig. 1E). With systematic analysis of FOLR2 expression by NLCs from 62 patient samples (Fig. S1C), we categorized PBMC cultures into three groups: FOLR2^{high} (MFI>4500, median=16258), FOLR2^{low} (1500<MFI<4500, median=3227) and FOLR2^{neg} (MFI<1500, median=340). The CLL cell viability among these three groups varied significantly (Fig.1F), being highest in the FOLR2^{high} (mean=94.2%, n=40) and the lowest in the FOLR2^{neg} (mean=56.3%, n=16). Furthermore, lack of NLCs led to significant decrease of viability of CLL cells from FOLR2^{high}, but not FOLR2^{neg} group (Fig. S1D). Next, we correlated the level of FOLR2 and other myeloid markers expressed by NLCs with survival of CLL cells in the PBMC cultures. Among 40 patient samples, FOLR2 had the strongest correlation with cancer cell survival (Fig. 1G; Fig. S1E), followed by CD163 and CD14 markers, while CD64 and CD86, showed a negative association with viability

of cancer cells. These results indicate that FOLR2$^+$ NLCs protect CLL cells from spontaneous apoptosis and identify FOLR2 as a specific marker of protective M2-like NLCs *in vitro*.

Finally, we tested the FOLR2 expression by NLCs in the lymph nodes (LNs) of CLL patients. Multiplex immunofluorescence (mIF) staining revealed a markedly higher expression of FOLR2 by CD163$^+$ NLCs in the CLL LNs, compared with the non-malignant ones (Fig. 1H). With these results we confirmed that NLCs in LNs of CLL patients are also expressing high level of FOLR2.

FOLR2 is detected on CLL cells co-cultured with NLCs

Given that CLL cells drive the maturation of FOLR2$^+$ NLCs, which in turn protect cancer cells from apoptosis, we wondered if FOLR2 could play a role in the interaction between these two cell types. During standard phenotyping of CLL PBMCs we detected myeloid markers: FOLR2, CD163, CD206 and CD14, on the big and granular NLCs (Fig. 2A, Fig. S2A). Surprisingly, gating on the remaining lymphoid cells revealed a subpopulation expressing myeloid markers (Fig. 2A), among which only FOLR2 was significantly detectable (Fig. 2B). Further analysis confirmed that FOLR2 is absent on of CD5$^+$/CD19$^+$ naïve CLL cells, and appears only after long-term PBMC culture (Fig. 2C), despite the lack of *FOLR2* gene expression by cancer cells (Fig. S2B).

These observations suggested that CLL cells acquired FOLR2 during PBMC cultures. To confirm whether CLL cells could acquire FOLR2 from NLCs, we performed *FOLR2* gene KO in NLCs (Fig. 2D). To generate sufficient NLC cells, we used a healthy donor NLCs system (HD-NLCs), where HD monocytes are co-cultured with CLL cells. These HD-NLCs correspond to NLCs in terms of functionality[9] and FOLR2 expression (Fig. S2C). *FOLR2* KO in HD-NLCs led to significant decrease in the percentage of FOLR2$^+$ CLL cells, as compared with the control condition (mean=0.95% vs 0.14%, n=11, p=0.006; Fig. 2E), confirming that NLCs are the source of the FOLR2 detected on CLL cells *in vitro*.

CLL cells acquire functional FOLR2 from NLCs through trogocytosis

Since CLL cells can engage in trogocytosis with NLCs[17], we investigated whether this mechanism could be responsible for acquisition of FOLR2 by cancer cells[31]. Using flow cytometry (FCM), we observed that CLL cells acquire PKH67-stained membranes and FOLR2 from NLCs, after 4h incubation (Fig. 3A). Across 15 samples, a mean of 20% and 2% of CLL cells were positive for PKH67 and FOLR2 respectively, while the signal from CD14 and CD16 was absent (Fig. 3B). Then, with confocal microscopy, we demonstrated direct interaction between FOLR2$^+$ NLCs and CD19$^+$ CLL cells (Fig. 3C) and detected CLL cells with FOLR2 patches co-localized with their plasma membranes (Fig. 3D and S3A), upon co-cultures with control HD-NLCs, but not *FOLR2*-KO HD-NLCs (Fig. 3E). These results demonstrate that CLL cells obtain FOLR2 from NLCs by trogocytosis and that the transfer is partially selective.

To test whether the FOLR2 acquired by CLL cells is functional, we incubated the co-cultures with EC17, a folic acid-FITC (FA-FITC) imaging agent[32]. Expectedly, FOLR2$^+$ NLCs showed high intracellular EC17 signals. As for CD19$^+$ CLL cells, we observed some with FOLR2 positive membrane patches and intracellular EC17 signal (Fig. 3F). On the other hand, CLL cells co-cultured with *FOLR2* KO NLCs lacked the FOLR2 signal and showed greatly reduced EC17 signal (Fig. 3F, bottom). Moreover, only CLL cells purified after the co-culture with CTRL HD-NLCs, but not *FOLR2* KO HD-NLCs were positive for EC17 (Fig. 3G) Finally, using FCM, we showed that FOLR2$^+$ CLL cells acquire more fluorescent-FA, compared to remaining cancer cells, which diminished in the presence of excess FA (Fig. S3C).

These results demonstrate that FOLR2 acquired by CLL cells is functional, facilitating uptake of folates independently on the presence of NLCs.

Trogocytic FOLR2$^+$ CLL cells are predominantly activated

Next, we studied the effect of trogocytosis on CLL cells during their activation and proliferation, induced by soluble factors[29–31]. First, we optimized the HD-NLC co-culture conditions to maximize CLL cells activation and FOLR2 trogocytosis (Fig. S4A). We tested IL-2+CpG[29] and CD40L[1]+IL-15[29,32,33] activation to compare the effect of more TLR- and BCR-centric protocols respectively. We chose CD40L+IL-15 treatment, as it led to NLC-dependent activation of CLL cells with efficient upregulation of CD23[34] and downregulation of CD184[35] (Fig. S4B_A), and significantly increased acquisition of FOLR2 by CLL cells (1.6% vs 5%, p=0.0315, n=6; fig. S4B_B). Next, we evaluated effect of initial HD-NLCs in the co-culture on FOLR2 acquisition by CLL cells. We observed that increase of HD-NLCs number from 5 to 10% leads to significant increase of FOLR2 acquisition of by CLL cells (2 vs 8%, p<0.0001, n=7, Fig. S4C).

For subsequent experiments we combined the optimized culture conditions, by incorporation of an additional cytokine priming and medium exchange to minimize the effects of nutrient depletion (Fig. 4A). Moreover, we added further surface markers to evaluate activation status of CLL cells, CD49d[36,37] and CD58 [18,42]. With the optimized protocol, we confirmed increased expression of activation markers: CD23, CD49d, CD58, and decreased expression of CD184 by CLL cells co-cultured with HD-NLCs, as compared with CLL monocultures (Fig. 4B). Furthermore, we observed a significantly increased frequency of FOLR2$^+$ trogocytic CLL cells with CD40L+IL-15 treatment (9 vs 40%, p=<0.0001, n=26; Fig. 4C), representing roughly a 10-fold increase as compared with a basic activation protocol (Fig. S4B). Moreover, the CD40L+IL-15 treatment led to the detection of other myeloid markers by cancer cells, CD11b and CD14 (Fig. S4F). Plotting FOLR2 signal against CLL activation markers demonstrated that the FOLR2$^+$ cell population is more likely found in the activated fraction of the cells, with high expression of CD23, CD49d, CD58 and low expression of CD184 (Fig. 4D). We further supported these findings, by confirming a significant correlation between FOLR2 enrichment score ($ES_{FORL2;}$ Fig.S4E_A) and the total percentage of CLL cells positive for a specific activation marker (p=<0.001, n=150; Fig. 4E).

Taken together, these results demonstrate that CD40L+IL-15 stimulation greatly promotes acquisition of FOLR2 by CLL cells, and that FOLR2$^+$ trogocytic CLL cells are enriched in the fraction of activated cells.

FOLR2$^+$ CLL cells are predominant subpopulation of proliferating cancer cells

To explore the relation of FOLR2 acquisition and proliferation, we compared the expression of Ki67 by CD40L+IL-15 treated CLL cells cultured alone or with HD-NLCs. We observed that the presence of HD-NLCs leads to induction of Ki67 expression by CLL cells, predominantly in the FOLR2$^+$/CD23$^+$/CD184^{low} subpopulations (Fig. 5A), which was consistent for 17 biological replicates (p<0.0001; samples from 12 patients; Fig. 5B). Furthermore, IL-15 turned out to be crucial in inducing an efficient Ki67 expression (Fig. S5B). Moreover, we observed a strong correlation between Ki67 enrichment score ($ES_{Ki67;}$ Fig.S4E) and the total fraction of Ki67$^+$ CLL cells (r=0.935, p<0.0001; Fig. 5C). Since Ki67 expression is specific mostly to actively cycling cells[43], we also performed dye-dilution assay using CellTrace™ Violet (CTV) to evaluate the

total percentage of proliferating cells, and confirmed significantly increased proportion of cells after division, after activation in the presence of HD-NLCs (4 vs 21%, p=0.0041, n=8; Fig. 5D).
To evaluate the effect of folic acid (FA) availability on the cell proliferation, we tested three culture conditions with decreasing FA content, FA^{high} (>1000µg/L), FA^{low} (~1.22µg/L) and $FA^{negative}$ (~0µg/L), using CLL cells that previously showed high proliferation. We observed, that reduction of FA leads to decrease of Ki67 expression and CTV dilution in CLL cells (Fig. 5E). After 6 days post-activation we observed around 40% vs 30% of $Ki67^{+}$ cells in FA^{high} and FA^{low} respectively, while in $FA^{negative}$ this value was below 1%, signifying lack of actively proliferating cells (p<0.001, n=6; Fig. 5E left). As for the CTV dilution assay, we confirmed that deprivation of FA causes significant decrease in CLL cell proliferation (p<0.05, n=6, Fig. 5E right). Nevertheless, even under $FA^{negative}$ conditions approximately 20% of cancer cells had undergone cell division.

$FOLR2^{+}$ CLL cells have a proliferative advantage under folic acid deprivation.

Subsequently, we evaluated if trogocytic $FOLR2^{+}$ CLL cells have an advantage in proliferation during scarcity of FA. We combined the results of Ki67 and CTV staining and studied the distribution of $FOLR2^{+}$ cells in the subpopulation of actively cycling CLL cells. We chose a patient with highly proliferative cells, capable of multiple cell division over the course of the experiment (Fig. 5F). Based on CTV staining alone, we observed a diminishing number of CTV peaks following a decrease in FA content in the media. When looking at CTV and Ki67 signals combined, we could differentiate the four cell populations, corresponding to: P1. $CTV^{high}Ki67^{-}$, quiescent cells that did not divide; P2. $CTV^{high}Ki67^{+}$, cells right before the first division; P3. $CTV^{low}Ki67^{+}$, subsequent generations of actively cycling cells; P4. $CTV^{low}Ki67^{-}$, cells after cycling, quiescent again. As for FOLR2 expression, it peaked in P2, declined slightly in P3, and dropped further in P1 and P4, mirroring Ki67 fluctuations. The effect was more pronounced under FA^{low} conditions. CD23 and CD184 levels showed a similar pattern. Moreover, we detected some $CD14^{+}$ CLL cells only in P2. Finally, by analyzing the subsequent cell generations of actively cycling cells (P3) we observed a stable level of FOLR2 (Fig. 5G), indicating that these cells performed multiple rounds of trogocytosis, since FOLR2 levels drop proportionally after each cell division.

These experiments demonstrated that NLCs play a crucial role in CD40L/IL-15-mediated CLL cell proliferation *in vitro*, and that $FOLR2^{+}$ trogocytic CLL cells are the predominant population of actively cycling CLL cells in HD-NLCs co-cultures. Cell cultures with decreasing concentration of FA confirmed that trogocytic $FOLR2^{+}$ CLL cells have a proliferative advantage under FA depletion, as compared to $FOLR2^{-}$ cancer cells.

Detection of trogocytic $FOLR2^{+}$ CLL cells in the lymph nodes of CLL patients

Finally, we investigated the relation between FOLR2 expression by NLCs and CLL cells proliferation, using mIF staining of whole LN sections from CLL patients.

First, based on FOLR2 and CD163 staining and the spatial distribution of NLCs, we detected 4 subpopulations of these cells: N1 ($FOLR2^{++}/CD163^{+}$), N2 ($FOLR2^{+}/CD163^{-}$), N3 ($FOLR2^{-}/CD163^{++}$) found with varying frequency in sub-capsular areas and lymphatic sinuses, and N4 ($FOLR2^{+++}CD163^{+++}$) located densely around the vascular structures (p<0.0001, n=21; Fig. 6A).

Aside from FOLR2$^+$ NLCs, we also detected the presence of CD20$^+$ CLL cells with patches of FOLR2 signal in plasma membrane and cytoplasm of the cells (Fig. 6B), suggesting a presence of trogocytic cancer cells, previously observed in vitro. Some of these FOLR2$^+$ CLL cells were also Ki67$^+$.

Since we could not confirm the enrichment of the trogocytic FOLR2$^+$ CLL cells in the fraction of proliferating cells, we investigated the potential relation between the frequency of FOLR2$^+$ NLCs (N1, N2 and N4) and the overall percentage of Ki67$^+$ CLL cells in the LNs. First, we noticed that the P1 and P2 subpopulations of NLCs are tightly intertwined with proliferating CLL cells (Fig. 6C). Then, we analyzed the LNs from 21 patients, and based on percentage of Ki67$^+$ cancer cells, we divided the samples into low and high proliferation groups with <10% Ki67$^+$ and >10% Ki67$^+$ CLL cells respectively (Fig. 6D). Comparison of the FOLR2$^+$ NLCs (N1, N2 and N4) percentage between these two groups revealed their significantly higher abundance in the samples with increased proliferation of CLL cells.

Observation of FOLR2$^+$ CLL cells in LNs confirmed that trogocytosis with NLCs occurs *in vivo*. Finally, a positive association of the frequency of FOLR2$^+$ NLCs with increased proliferation of CLL cells further enforced the importance of these cells in supporting cancer cell expansion.

DISCUSSION

The direct cell interactions are critical in the NLC-dependent support of CLL cell[1,7,17] . Nevertheless, the full extent of these interactions remains understudied, especially regarding their elusive nature and technological limitations[38]. Previously, we showed that trogocytic interaction between CLL cells and NLCs is important for the survival of cancer cells *in vitro*[17]. Here, we discovered that CLL cells use trogocytosis to acquire functional FOLR2 from NLCs, to increased their capacity for folic acid uptake. Additionally, FOLR2$^+$ CLL cells are predominantly detected in the fraction of activated and proliferating cancer cells *in vitro*. Moreover, detection of FOLR2$^+$ CLL cells in the LNs of the patients, and correlation between the percentage of FOLR2$^+$ NLCs and cancer cell proliferation**,** further supports the relevance of trogocytosis-mediated acquisition of FOLR2 by CLL cells

FOLR2, thanks to its high affinity, and rapid turnover[25,40,41], gives the trogocytic CLL cells an advantage in the uptake of folates. Folates are essential fuel for one-carbon metabolism, impacting nucleic acid, lipids and amino acids synthesis, necessary for cell growth and proliferation[27]. This would partially explain why FOLR2$^+$ trogocytic CLL cells belong to the predominant population of activated and proliferating cancer cells *in vitro,* especially during folate scarcity. Moreover, we demonstrated that the actively cycling population of CLL cells *in vitro* is characterized by a constant level of extracellular FOLR2, which drops as soon as they become quiescent again. This implies that CLL cells engage in trogocytosis with NLCs between each cell cycle and potentially use FOLR2 to sustain their increased folate demands. These findings are supported by our observation that CLL cells remain in close contact with FOLR2$^+$ NLCs in the CLL LNs, and that during CLL progression, NLCs show an increased infiltration into proliferation centers[4], hence being more accessible for the actively proliferating CLL cells. In the literature, there are similar examples of trogocytic cells, gaining increased adaptability. For instance, Lu et al. demonstrated that healthy NK cells, can acquire a tyrosine kinase receptor TYRO3 from tumor cells, resulting in their increased activation and proliferation[39].

With our results, we observed a certain selectivity of the protein transfer during the CLL-NLC trogocytic interaction. Out of the tested proteins, FOLR2 is the main NLC-derived protein detectable on CLL cells in the resting conditions. FOLR2 is a small, GPI-anchored protein located on the plasma membrane (PM) of NLCs. On the other hand, CD16, CD163 and CD206, which show negligible acquisition by CLL cells, are all integral transmembrane proteins, with stronger association to the PM[42]. This suggests that, in

resting conditions, trogocytosis encompasses only the outer layer of the NLC PM. On the other hand, CD14 is also a small GPI-anchored protein, predominantly co-expressed with FOLR2, yet showing much smaller transfer, and retention by CLL cells, which further indicates the selectivity and importance of FOLR2 transfer. We could speculate that CLL PM contains molecules that stabilize interaction with FOLR2, resulting in its higher acquisition and retention. Moreover, upon CD40L+IL-15 priming, we observed not only a 10-fold increase in the transfer of FOLR2 to cancer cells, but also a substantial acquisition of CD11b and CD14, suggesting that this activation is intensifying interaction between CLL cells and NLCs, and thus the trogocytosis process itself. It has been shown previously that FOLR2 inhibits the CD11b/CD18-mediated adhesion of macrophages to collagen[43], and so it might be also implicated in regulating the interaction between NLCs and CLL cells.

Besides further characterization of the CLL-NLC trogocytic interaction, we defined FOLR2 as ultimate marker of NLCs, allowing to discriminate between protective and non-protective phenotypes *in vitro.* Moreover, we demonstrated the presence of different NLCs subpopulations varying in CD163 and FOLR2 expression in CLL LNs, and observed that the FOLR2-expressing NLCs subset was correlated with proliferating CLL cells. Besides, we distinguished a population of NLCs highly associated with vasculature, which was characterized with especially high expression of FOLR2. We speculated that this group of NLCs might be responsible for homing the CLL cells to the lymphoid organs[1]. These results highlight previously unknown heterogeneity of NLCs, stressing the importance of further characterization of these peculiar cells**.**

While the FOLR2 expressing NLCs seem to be a crucial element of CLL TME, the exact role of FOLR2 in these cells as well as other TAMs remains speculative. According to the literature, expression of FOLR2 may lead to accumulation of folates in macrophages, supporting epigenetic changes that stabilize the immunosuppressive phenotype of these cells[26]. This stays in agreement with the results by Vaca et al., demonstrating that NLCs are highly immunosuppressive cells, promoting expansion of T helper cells, and further hindering immune responses against cancer cells[44]. Moreover, following the observation of folic acid transfer from NLCs to CLL cells, we speculate that FOLR2^{high} NLCs could act as a reservoir of folates for the cancer cells in the lymphoid organs. This could be especially relevant during the active phase of the disease, when the concentration of this vitamin might become a limiting factor for cell proliferation[26]. Nevertheless, the acquisition of FOLR2 by CLL cells cannot fully account for the beneficial effect of trogocytosis regarding cell activation and proliferation. Already, based on PKH67 staining we observed that FOLR2^{+} CLL cells represent only a fraction of the total population of trogocytic cells, which acquire also other components of NLCs plasma membrane. Other researchers proposed that trogocytosis could help cells gain lipids necessary for cell proliferation[18].Lipids represent especially energy-demanding building blocks for the proliferating cells[45], so the possibility to incorporate NLC-derived membranes by trogocytic CLL cells could further optimize their metabolic demands.

This work underlies the central role of FOLR2^{+} NLCs in supporting CLL cells, and characterizes a novel, trogocytosis-mediated type of pro-tumoral interaction between these two cell types. Trogocytosis remains an elusive phenomenon, with many challenges regarding the description of its exact extent and role in cancer progression. We believe that uncovering the intricacy of trogocytosis in CLL could increase our understanding of the cancer cell interactions within the TME, leading to more efficient therapeutic strategies, potentially relevant for other types of cancers.

Acknowledgments

The authors thank the many patients who generously donated clinical samples for this study. This work was supported in part by the Janssen Foundation, Région Midi-Pyrénées, La Ligue Nationale Contre le Cancer, CNRS, and Toulouse III University. We would like to thank the members of the platform IMAG'IN (l'Institut Universitaire du Cancer de Toulouse), especially N. Van Acker, FX. Frenois and A. Belin-Artola for the IHC staining of LN. We are grateful to P. Gravelle for facilitating communication with the Anatomo-Pathology Department of the IUCT Oncopole and to A. Quillet-Mary for her critical review of the manuscript. Schematics were created using BioRender.com.
Institutional Review Board Statement: The study was conducted according to the guidelines of the Declaration of Helsinki, and approved by the Institutional Review Board (or Ethics Committee) of INSERM (protocol code DC-2013-1903 and date of approval 2013).

Authorship

Contribution: M.D. designed the study, performed the experiments, interpreted data, and wrote the manuscript; B.G. participated in design of the research; C.B. processed the healthy-donor blood samples. L.Y. provided patients' blood samples and associated clinical data; C.L. provided the patients' lymph node samples, associated clinical data, and supervised IHC staining; V.P. provided the funding; M.P provided the funding, designed the study, interpreted data and wrote the manuscript. All the authors critically reviewed the manuscript.

Conflict-of-interest disclosure: the authors declare no conflict of interest.

For original data, please contact the corresponding authors.

Bibliography

1. Kipps TJ, Stevenson FK, Wu CJ, et al. Chronic lymphocytic leukaemia. *Nat Rev Dis Primers*. 2017;3(Cll). doi:10.1038/nrdp.2016.96
2. Lapieaux L, Delforfe A, Bron P, De Bruyn C, Slryckmans P. Chronic lymphocytic leukemia (CLL) B-lymphocytes but not normal B-lymphocytes are rescued from apoptosis by contact with bone marrow stromal cells. *Exp Hematol*. 1997;25(8):862. doi:10.1182/blood.V91.7.2387
3. Burger JA, Quiroga MP, Hartmann E, et al. High-level expression of the T-cell chemokines CCL3 and CCL4 by chronic lymphocytic leukemia B cells in nurselike cell cocultures and after BCR stimulation. *Blood*. 2009;113(13):3050-3058. doi:10.1182/blood-2008-07-170415
4. Boissard F, Laurent C, Ramsay AG, et al. Letter to the editor: Nurse-like cells impact on disease progression in chronic lymphocytic leukemia. *Blood Cancer J*. 2016;6(1). doi:10.1038/bcj.2015.108
5. Zaaboub R, Vimeux L, Contremoulins V, et al. Nurselike cells sequester B cells in disorganized lymph nodes in chronic lymphocytic leukemia via alternative production of CCL21. *Blood Adv*. 2022;6(16):4691-4704. doi:10.1182/bloodadvances.2021006169
6. Guo Y, Pei H, Lu B, et al. Aberrantly expressed Wnt5a in nurse-like cells drives resistance to Venetoclax in chronic lymphocytic leukemia. *Cell Death Discov*. 2022;8(1):1-9. doi:10.1038/s41420-022-00884-y
7. Koehrer S, Burger JA. Chronic Lymphocytic Leukemia: Disease Biology. *Acta Haematol*. 2024;147(1):9-23. doi:10.1159/000533610
8. Burger JA, Tsukada N, Burger M, Zvaifler NJ, Dell'Aquila M, Kipps TJ. Blood-derived nurse-like cells protect chronic lymphocytic leukemia B cells from spontaneous apoptosis through stromal cell-derived factor-1. *Blood*. 2000;96(8):2655-2663. doi:10.1182/blood.v96.8.2655
9. Tsukada N, Burger JA, Zvaifler NJ, Kipps TJ. Distinctive features of "nurselike" cells that differentiate in the context of chronic lymphocytic leukemia. *Blood*. 2002;99(3):1030-1037. doi:10.1182/blood.V99.3.1030
10. Chen Y, Chen L, Yu J, et al. Cirmtuzumab blocks Wnt5a/ROR1 stimulation of NF-kB to repress autocrine STAT3 activation in chronic lymphocytic leukemia. *Blood*. 2019;134(13):1084-1094. doi:10.1182/blood.2019001366
11. Boissard F, Fournié JJ, Quillet-Mary A, Ysebaert L, Poupot M. Nurse-like cells mediate ibrutinib resistance in chronic lymphocytic leukemia patients. *Blood Cancer J*. 2015;5:e355. doi:10.1038/bcj.2015.74
12. Ysebaert L, Fournié JJ. Genomic and phenotypic characterization of nurse-like cells that promote drug resistance in chronic lymphocytic leukemia. *Leuk Lymphoma*. 2011;52(7):1404-1406. doi:10.3109/10428194.2011.568078
13. Jia L, Clear A, Liu FT, et al. Extracellular HMGB1 promotes differentiation of nurse-like cells in chronic lymphocytic leukemia. *Blood*. 2014;123(11):1709-1719. doi:10.1182/blood-2013-10-529610
14. Talbot H, Saada S, Barthout E, et al. BDNF belongs to the nurse-like cell secretome and supports survival of B chronic lymphocytic leukemia cells. *Sci Rep*. 2020;10(1):1-9. doi:10.1038/s41598-020-69307-1
15. Elisa ten Hacken 1, Maria Gounari, 2, 3 Jaap Willem Back 4, Ekaterina Shimanovskaya 4, et al. Calreticulin as a novel B-cell receptor antigen in chronic lymphocytic leukemia. *J ECT*. 2011;27(2):175-177. doi:doi:10.3324/haematol.2017.169102
16. Deaglio S, Vaisitti T, Bergui L, et al. CD38 and CD100 lead a network of surface receptors relaying positive signals for B-CLL growth and survival. *Blood*. 2005;105(8):3042-3050. doi:10.1182/blood-2004-10-3873
17. Boissard F, Tosolini M, Ligat L, et al. Nurse-like cells promote CLL survival through LFA-3/CD2 interactions. *Oncotarget*. 2017;8(32):52225-52236. doi:10.18632/oncotarget.13660
18. Joly E, Hudrisier D. What is trogocytosis and what is its purpose? *Nat Immunol*. 2003;4(9):815. doi:10.1038/ni0903-815
19. Schriek P, Ching AC, Moily NS, et al. Marginal zone B cells acquire dendritic cell functions by trogocytosis. *Science (1979)*. 2022;375(6581). doi:10.1126/science.abf7470

20. Shin JH, Jeong J, Maher SE, Lee HW, Lim J, Bothwell ALM. Colon cancer cells acquire immune regulatory molecules from tumor-infiltrating lymphocytes by trogocytosis. *Proc Natl Acad Sci U S A*. 2021;118(48). doi:10.1073/pnas.2110241118
21. Kawashima M, Higuchi H, Kotani A. Significance of trogocytosis and exosome-mediated transport in establishing and maintaining the tumor microenvironment in lymphoid malignancies. *Journal of Clinical and Experimental Hematopathology*. 2021;61(4):192-201. doi:10.3960/jslrt.21005
22. Cresswell GM, Wang B, Kischuk EM, et al. Folate Receptor Beta Designates Immunosuppressive Tumor-Associated Myeloid Cells That Can Be Reprogrammed with Folate-Targeted Drugs. *Cancer Res*. 2021;81(3):671-684. doi:10.1158/0008-5472.CAN-20-1414
23. Xia W, Hilgenbrink AR, Matteson EL, Lockwood MB, Cheng JX, Low PS. A functional folate receptor is induced during macrophage activation and can be used to target drugs to activated macrophages. *Blood*. 2009;113(2):438-446. doi:10.1182/blood-2008-04-150789
24. Zhang F, Huang B, Utturkar SM, et al. Tumor-specific activation of folate receptor beta enables reprogramming of immune cells in the tumor microenvironment. *Front Immunol*. 2024;15(February):1-14. doi:10.3389/fimmu.2024.1354735
25. Rafael Samaniego 1,* , Ángeles Domínguez-Soto 2,*, Manohar Ratnam 3, Takami Matsuyama 4, Paloma Sánchez-Mateos 5, Ángel L. Corbí 2,† and Amaya Puig-Kröger 6 †. Folate Receptor β (FRβ) Expression in Tissue-Resident and Tumor-Associated Macrophages Associates with and Depends on the Expression of PU.1. Published online 2020:1-17.
26. Samaniego R, Palacios BS, Domiguez-Soto Á, et al. Macrophage uptake and accumulation of folates are polarization-dependent in vitro and in vivo and are regulated by activin A. *J Leukoc Biol*. 2014;95(5):797-808. doi:10.1189/jlb.0613345
27. Ducker GS, Rabinowitz JD. One-Carbon Metabolism in Health and Disease. *Cell Metab*. 2017;25(1):27-42. doi:10.1016/j.cmet.2016.08.009
28. Domagala M, Ysebaert L, Ligat L, et al. IL-10 rescues CLL survival through repolarization of inflammatory nurse-like cells. *Cancers (Basel)*. 2022;14(1):1-15. doi:10.3390/cancers14010016
29. Schleiss C, Ilias W, Tahar O, et al. BCR-associated factors driving chronic lymphocytic leukemia cells proliferation ex vivo. *Sci Rep*. 2019;9(1):1-12. doi:10.1038/s41598-018-36853-8
30. Sun C, Chen YC, Zurita AM, et al. The immune microenvironment shapes transcriptional and genetic heterogeneity in chronic lymphocytic leukemia. *Blood Adv*. 2023;7(1):145-158. doi:10.1182/bloodadvances.2021006941
31. Ghamlouch H, Ouled-Haddou H, Damaj G, Royer B, Gubler B, Marolleau JP. A Combination of Cytokines Rescues Highly Purified Leukemic CLL B-Cells from Spontaneous Apoptosis In Vitro. *PLoS One*. 2013;8(3):1-9. doi:10.1371/journal.pone.0060370
32. De Totero D, Meazza R, Capaia M, et al. The opposite effects of IL-15 and IL-21 on CLL B cells correlate with differential activation of the JAK/STAT and ERK1/2 pathways. *Blood*. 2008;111(2):517-524. doi:10.1182/blood-2007-04-087882
33. Gupta R, Li W, Yan XJ, et al. Mechanism for IL-15–Driven B Cell Chronic Lymphocytic Leukemia Cycling: Roles for AKT and STAT5 in Modulating Cyclin D2 and DNA Damage Response Proteins. *The Journal of Immunology*. 2019;202(10):2924-2944. doi:10.4049/jimmunol.1801142
34. Takács F, Tolnai-Kriston C, Hernádfői M, et al. The Effect of CD86 Expression on the Proliferation and the Survival of CLL Cells. *Pathology and Oncology Research*. 2019;25(2):647-652. doi:10.1007/s12253-018-0512-7
35. Pozzo F, Forestieri G, Vit F, et al. Early reappearance of intraclonal proliferative subpopulations in ibrutinib-resistant chronic lymphocytic leukemia. *Leukemia*. 2024;38(8):1712-1721. doi:10.1038/s41375-024-02301-y
36. Bulian P, Shanafelt TD, Fegan C, et al. CD49d is the strongest flow cytometry-based predictor of overall survival in chronic lymphocytic leukemia. *Journal of Clinical Oncology*. 2014;32(9):897-904. doi:10.1200/JCO.2013.50.8515
37. Burger M, Hartmann T, Krome M, et al. Small peptide inhibitors of the CXCR4 chemokine receptor (CD184) antagonize the activation, migration, and antiapoptotic responses of CXCL12 in chronic lymphocytic leukemia B cells. *Blood*. 2005;106(5):1824-1830. doi:10.1182/blood-2004-12-4918
38. Bechtel TJ, Reyes-Robles T, Fadeyi OO, Oslund RC. Strategies for monitoring cell–cell interactions. *Nat Chem Biol*. 2021;17(6):641-652. doi:10.1038/s41589-021-00790-x

39. Lu T, Ma R, Li Z, et al. Hijacking TYRO3 from tumor cells via trogocytosis enhances NK-cell effector functions and proliferation. *Cancer Immunol Res*. 2021;9(10):1229-1241. doi:10.1158/2326-6066.CIR-20-1014
40. Puig-Kröger A, Sierra-Filardi E, Domínguez-Soto A, et al. Folate receptor β is expressed by tumor-associated macrophages and constitutes a marker for M2 anti-inflammatory/regulatory Macrophages. *Cancer Res*. 2009;69(24):9395-9403. doi:10.1158/0008-5472.CAN-09-2050
41. Gutiérrez-Seijo A, García-Martínez E, Barrio-Alonso C, et al. Activin A Sustains the Metastatic Phenotype of Tumor-Associated Macrophages and Is a Prognostic Marker in Human Cutaneous Melanoma. *Journal of Investigative Dermatology*. 2022;142(3):653-661.e2. doi:10.1016/j.jid.2021.07.179
42. Yu S, Guo Z, Johnson C, Gu G, Wu Q. Recent progress in synthetic and biological studies of GPI anchors and GPI-anchored proteins. *Curr Opin Chem Biol*. 2013;17(6):1006-1013. doi:10.1016/j.cbpa.2013.09.016
43. Machacek C, Supper V, Leksa V, et al. Folate Receptor β Regulates Integrin CD11b/CD18 Adhesion of a Macrophage Subset to Collagen. *The Journal of Immunology*. 2016;197(6):2229-2238. doi:10.4049/jimmunol.1501878
44. Vaca AM, Ioannou N, Sivina M, et al. Activation and expansion of T-follicular helper cells in chronic lymphocytic leukemia nurselike cell co-cultures. *Leukemia*. 2022;36(5):1324-1335. doi:10.1038/s41375-022-01519-y
45. Snaebjornsson MT, Janaki-Raman S, Schulze A. Greasing the Wheels of the Cancer Machine: The Role of Lipid Metabolism in Cancer. *Cell Metab*. 2020;31(1):62-76. doi:10.1016/j.cmet.2019.11.010

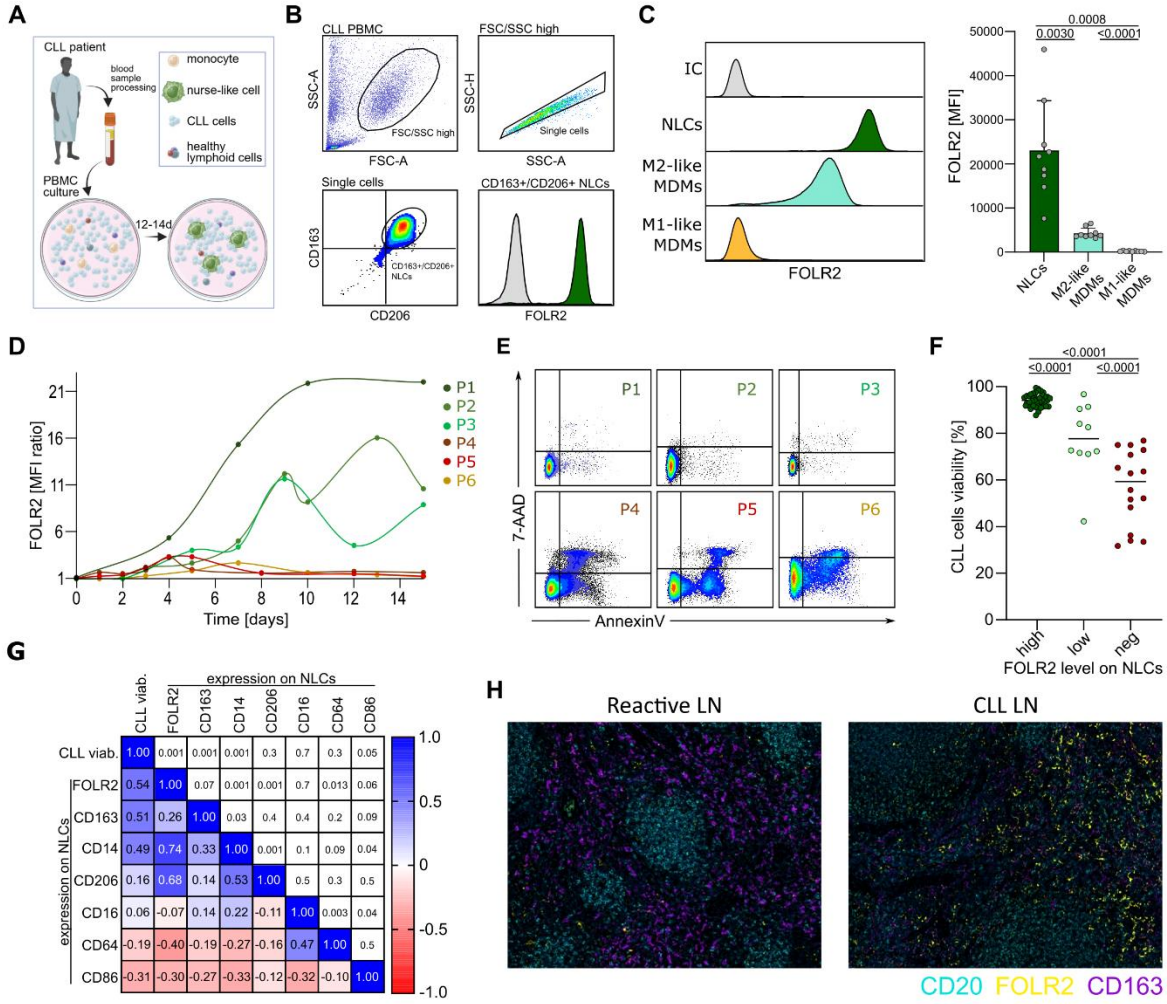

Figure 1. FOLR2 is a marker of protective NLCs. Scheme of generation of NLCs from CLL PBMC culture *in vitro*. **A)** FC analysis of the expression of FOLR2 on a subpopulation of NLCs ($CD163^{+}CD206^{+}$) generated in a culture of PBMC from a CLL patient (grey: isotypic control; green: anti-FOLR2). **B)** Comparison of FOLR2 expression on various types of *in vitro* generated macrophages: NLCs, M2-like and M1-like macrophages (Left: representative histograms; right: compilation of 9 independent experiments. **C)** Kinetics of FOLR2 expression during $CD14^{+}$ monocyte to NLC differentiation in CLL PBMC cultures for 14 days measured by FC (MFI ratio: anti-FOLR2/isotopic control). **D)** FC analysis of the CLL cells viability from CLL PBMC cultures on day 12 (annexin V/7-AAD staining). **E)** Percentage of CLL cells viability for the three groups of CLL patients according to the FOLR2 expression on NLCs. **F)** Correlation of the FOLR2 expression on NLCs with the CLL cells viability. **G)** Multiplex immunofluorescence (mIF) of a reactive lymph node and a lymph node from a CLL patient with the staining of CD20 (cyan), FOLR2 (yellow) and CD163 (purple). **H)** Representative images of lymph nodes from CLL patients, with various stages of the disease, from indolent to accelerated and Richter transformation; stained with anti-CD20 (cyan), anti-FOLR2 (yellow) and anti-CD163 (purple) antibodies (objective: x20).

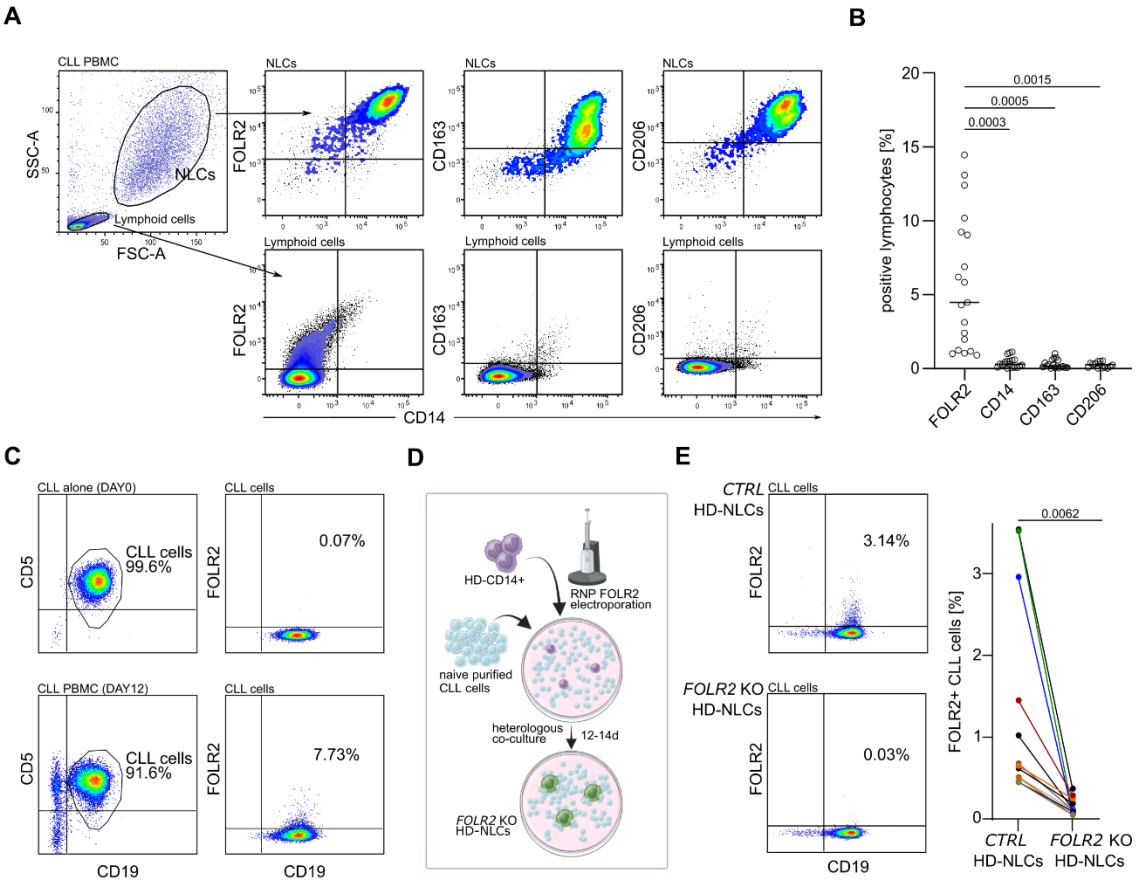

Figure 2. Detection of FOLR2 on the surface of CLL cells. A) FC analysis of the expression of FOLR2, CD14, CD163 and CD206 on cells from a culture of PBMC from a CLL patient at day 12 of *in vitro* culture, results for big, granular cells corresponding to NLCs (upper panel) and small cells corresponding to lymphoid cells (bottom panel). **B)** Expression of FOLR2, CD14, CD163, CD206 on the small cells (lymphocytes including CLL cells) of CLL PBMC cultures at day 12 (19 donors). **C)** FOLR2 expression on CLL cells ($CD5^{+}CD19^{+}$) alone at day 0 or in PBMC culture on day 12. **D)** left: FOLR2 expression by CLL cells in co-culture with CTRL HD-NLCs or FOLR2 KO NLCs; right: Percentage of $FOLR2^{+}$ CLL cells in co-cultures with CTRL HD-NLCs or *FOLR2* KO HD-NLCs (10 independent experiments).

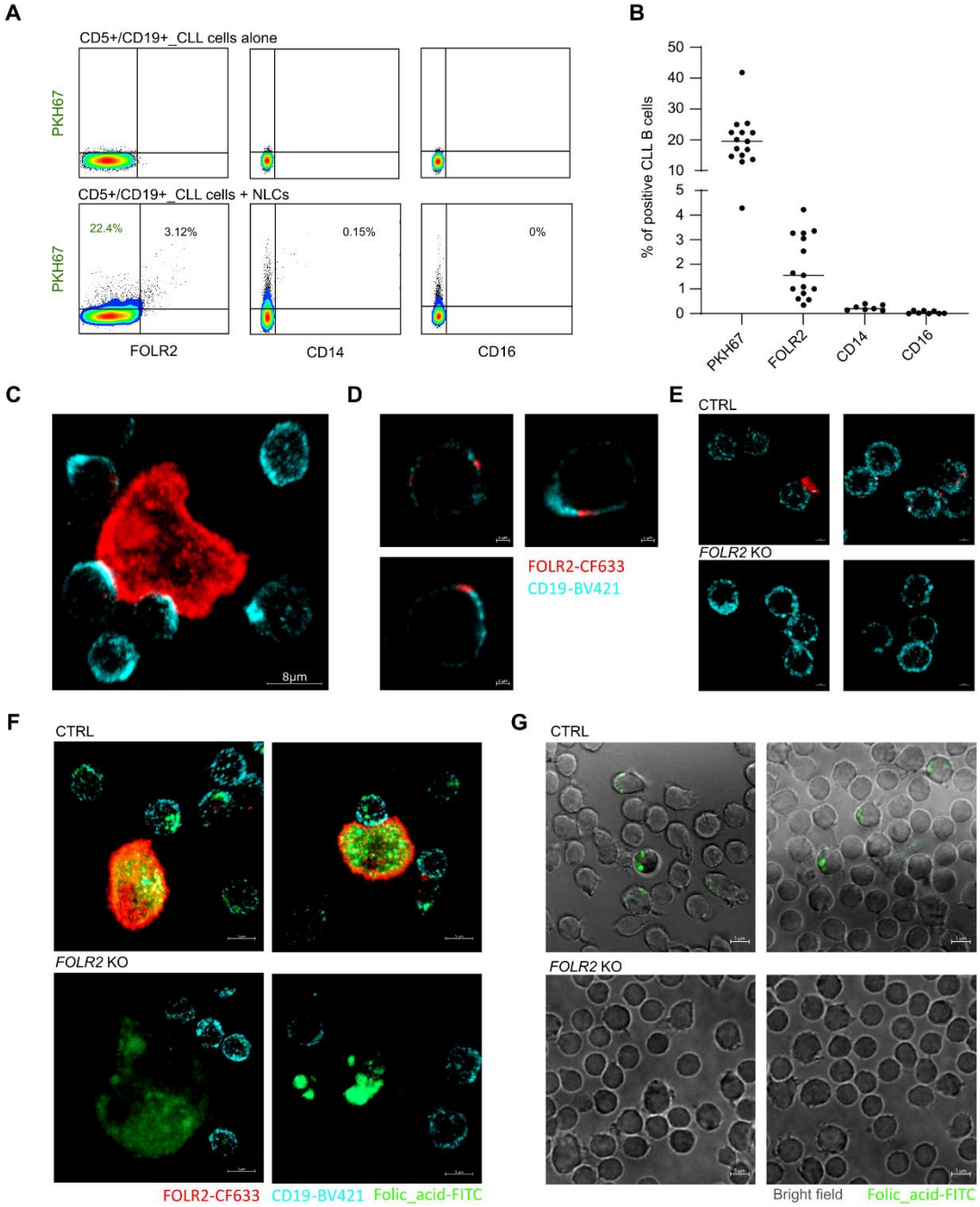

Figure 3. CLL cells acquire functional FOLR2 from NLCs by trogocytosis. A) FC analysis of the PKH67/FOLR2/CD14/CD16 signal on CLL cells after 4-hours of co-culture with PKH67^{+} NLCs (upper: CLL cells alone; below: co-culture with NLCs). **B)** Percentage of CLL cells positive for PKH67, FOLR2, CD14 and CD16 after 4-hours of co-culture with NLCs (15 independent experiments). **C-E)** Confocal microscopy (x63 magnification) of co-culture of CLL cells (CD19^{+}: cyan) and NLCs (FOLR2^{+}: red) during 4-hours showing: the contact of NLCs and CLL cells (**C**), the acquisition of FOLR2 patches by CLL cells after contact with NLCs (**D**) and the absence of detection of FOLR2 signal on CLL cells after co-culture with *FOLR2* KO HD-NLCs (**E**). **F)** Confocal microscopy of a 4-

hours co-culture of CLL cells with CTRL HD-NLCs (upper) or with FOLR2 KO NLCs (below) incubated with folic acid-FITC (green) then stained with anti-FOLR2-CF633 (red) and with CD19-BV421 (cyan). **G)** Confocal microscopy of purified CLL cells after co-culture with CTRL HD-NLCs (upper) or *FOLR2* KO HD-NLCs (below), following by incubation with folic acid-FITC for 90 min.

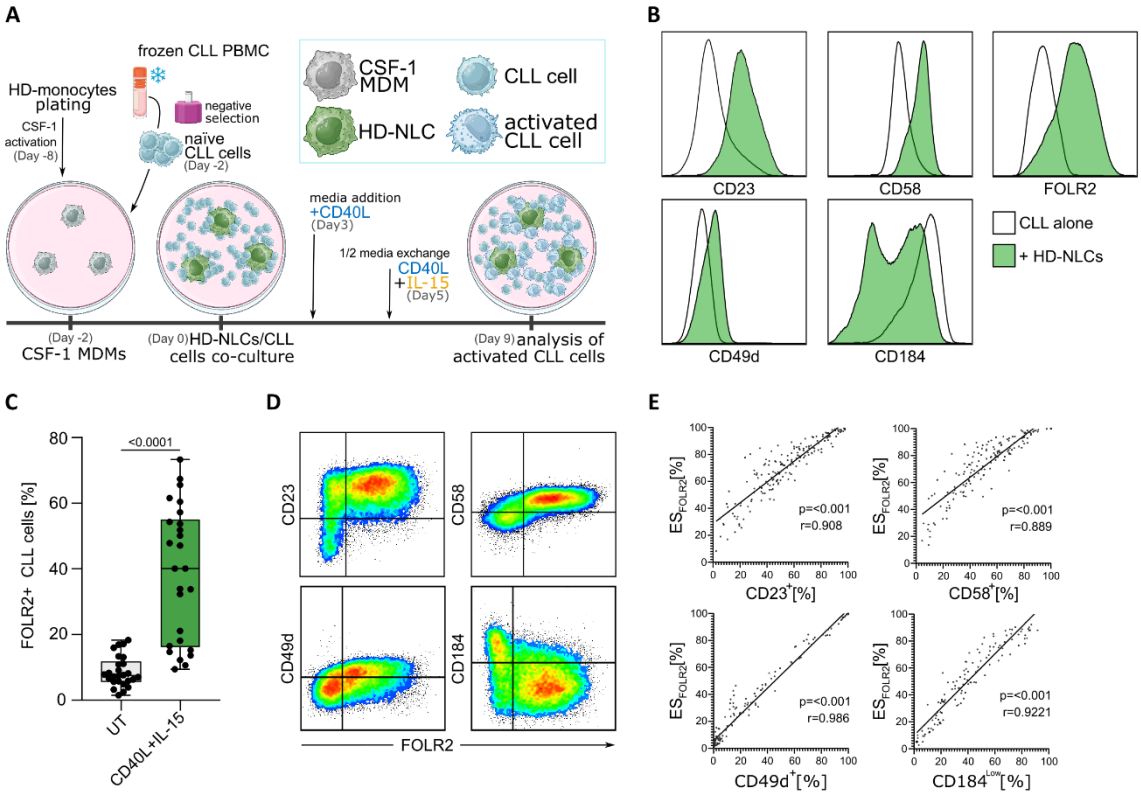

Figure 4. FOLR2 transfer is positively associated with activation of CLL cells. A) FC analysis of the CD23 and CD184 expression on CLL cells alone or in the presence of HD-NLCs incubated or not with IL-2+CpG or CD40L+IL-15 (left: one representative experiment; right: four independent experiments). **B)** Percentage of FOLR2$^+$ CLL cells analyzed by FC following co-culture with HD-NLCs in the presence or not of IL-2+CpG or CD40L+IL-15. **C)** Percentage of FOLR2$^+$ CLL cells after co-culture with increasing amount of NLCs: 5, 10 or 20%. **D)** FC analysis of expression of CD23, CD58, CD184, FOLR2, CD49d, CD5 and CD19 on CLL cells cultivated alone (white) or with HD- NLCs (green) in the presence of CD40L+IL-15. **E)** Percentage of FOLR2$^+$ CLL cells in co-culture with HD-NLCs in the presence or not of CD40L+IL-15. **F)** Expression of CD23, CD58, CD184, CD71, CD49d, and FOLR2 on CLL cells after co-culture with HD-NLCs in the presence of CD40+IL-15. **G)** Representation of the correlation between the total fraction of CLL cells positive for the different CLL markers (CD23, CD58, CD71, CD49d and CD184) and the percentage of FOLR2$^+$ cells expressing each of these markers (5 independent experiments, 12 patients, >200 samples).

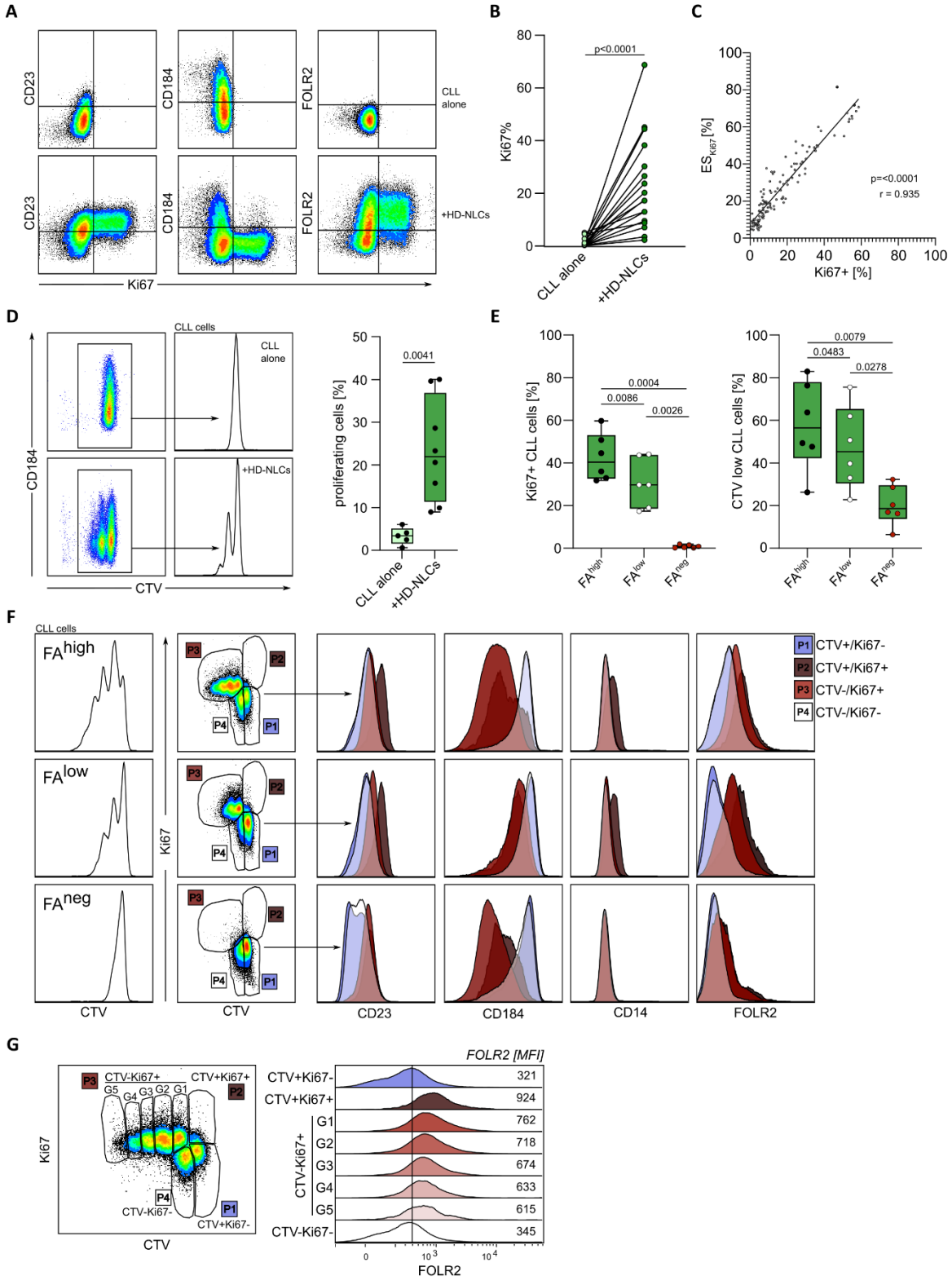

Figure 5 Trogocytic FOLR2⁺ CLL cells have an advantage in proliferation in FA deprived conditions. A) FC analysis of expression of Ki67, CD23, CD184 and FOLR2 on CLL cells cultured alone or with HD-NLCs in the presence of CD40L+Il15. **B)** Percentage of Ki67⁺ CLL cells cultured

alone or with HD-NLCs in the presence of CD40L+IL-15. **C)** Correlation between FOLR2 acquisition and Ki67 expression by CLL cells co-cultured with HD-NLCs in the presence of CD40L+IL-15 (5 independent experiments, 12 patients, >200 samples). **D)** CTV dilution assay of CLL cells cultured alone or with HD-NLCs in the presence of CD40L+IL-15: exemplary FC results (left), cumulative results from 8 patients represented as percentage of proliferating cells based on decrease in CTV signal (right). **E)** Percentage of actively cycling ($Ki67^{+}$, left) and total fraction of cycling (CTV low, right) CLL cells in co-culture with HD-NLCs in the presence of CD40L+IL-15, in the media with various concentrations of folic acid (FA). **F)** FC analysis of CD23, CD184, CD14 and FOLR2 signal on CLL cells stratified based on Ki67/CTV level (P1. $CTV^{high}Ki67^{-}$: quiescent cells that did not divide; P2. $CTV^{high}Ki67^{+}$: cells right before the first division; P3. $CTV^{low}Ki67^{+}$: actively cycling cells after previous division; P4. $CTV^{low}Ki67^{-}$: cells after cycling, quiescent again). **G)** FC analysis of FOLR2 level represented as MFI on CLL cells, depending on the proliferative status (Ki67/CTV) and subsequent cell generations (G1-G5).

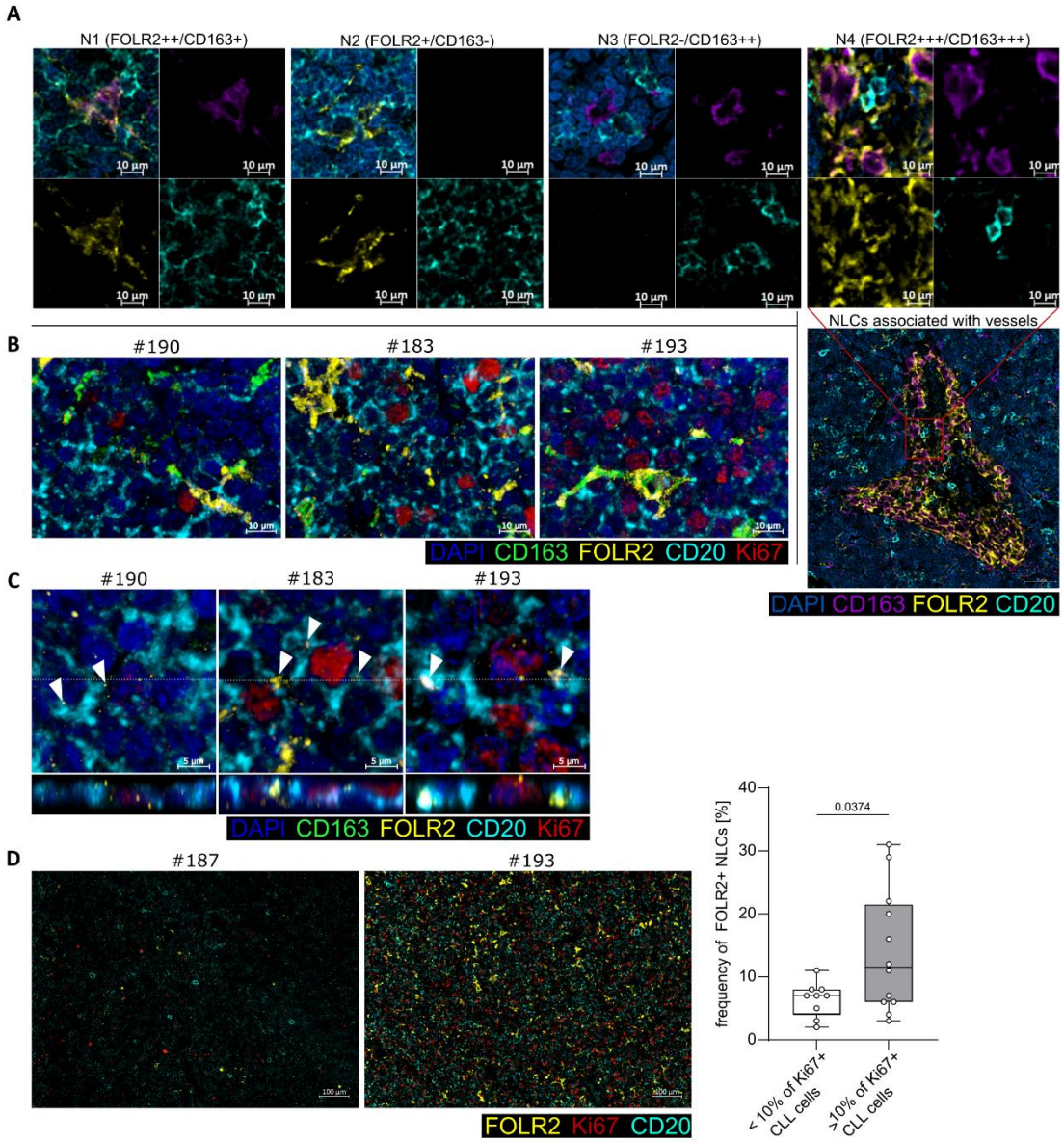

Figure 6 Detection of FOLR2⁺ CLL cells *in vivo* and correlation between FOLR2⁺ NLCs and CLL cells proliferation. CLL lymph node tissue sections (n=21 patients) of 4µm were stained with DAPI (blue) and anti-CD20 (cyan), anti-FOLR2 (yellow), anti-CD163 (purple), anti-Ki67 (red) antibodies, and visualized with confocal microscope (objective: x20). A) Left – representative images of 4 subgroups of NLCs, differentiated based on FOLR2 and CD163 expression: P1 ($FOLR2^+/CD163^+$), P2 ($FOLR2^+/CD163^-$), P3 ($FOLR2^-/CD163^+$), P4 ($FOLR2^{+++}CD163^{++}$) and association with vasculature (P4). Right – quantitative analysis of FOLR2 and CD163 MFI on different subgroups of NLCs. B) Detection of FOLR2 signal patches on $CD20^+$ CLL cells. C) $FOLR2^+/CD163^+$ NLCs are densely surrounded by $Ki67^+$ CLL cells. D) FOLR2+ NLCs are more frequent in the LNs where CLL cells have higher proliferative index.